Heat Mass Transfer
DOI 10.1007/s00231-017-2053-0

ORIGINAL

The dynamics of the water droplet impacting onto hot solid surfaces at medium Weber numbers

Windy H. Mitrakusuma[1,4] · Samsul Kamal[2,5] · Indarto[2,5] · M. Dyan Susila[3] · Hermawan[2] · Deendarlianto[2,5]

Received: 18 October 2016 / Accepted: 27 March 2017

Abstract The effects of the wettability of a droplet impacting onto a hot solid surface under medium Weber numbers were studied experimentally. The Weber numbers used in the present experiment were 52.1, 57.6, and 63.1. Three kinds of solid surfaces with different wettability were used. These were normal stainless steel (NSS), TiO_2 coated NSS, and TiO_2 coated NSS radiated with ultraviolet rays. The surface temperatures were varied from 60 to 200 °C. The image of side the view and 30° from horizontal were taken to explain the spreading and the interfacial behavior of a single droplet during impact the hot solid surfaces. It was found that under medium Weber numbers, the surface wettability plays an important role on the droplet spreading and evaporation time during the impact on the hot solid surfaces. The higher the wettability, the larger the droplet spreading on the hot surface, and the lower the evaporation time.

✉ Deendarlianto
deendarlianto@ugm.ac.id

[1] Department of Mechanical Engineering, Faculty of Engineering, Gadjah Mada University, Jl. Grafika No. 2, Yogyakarta 55281, Indonesia

[2] Department of Mechanical and Industrial Engineering, Faculty of Engineering, Gadjah Mada University, Jl. Grafika No. 2, Yogyakarta 55281, Indonesia

[3] Department of Mechanical Engineering, Lampung University, Jl. Prof. Dr. Sumantri Brojonegoro No. 1, Bandar Lampung, Indonesia

[4] Department of Refrigeration and Air Conditioning, Politeknik Negeri Bandung, Jl. Gegerkalong Hilir, Ds. Ciwaruga, Kotak Pos 1234, Bandung, Indonesia

[5] Centre for Energy Studies, Gadjah Mada University, Sekip K-1A Kampus UGM, Yogyakarta 55281, Indonesia

List of symbols

A	Surface area (m^2)
D, d	Diameter (m)
h	Latent heat of evaporation (kJ/kg)
q	Heat flux (W/m^2)
T	Temperature (°C, K)
Q	Heat (kJ)
u	Droplet velocity (m/s)
We	Weber number

Greek symbols

β	Spreading ratio
ρ	Density (kg/m^3)
σ	Surface tension (N/m)
θ	Contact angle (°)
τ	Evaporation time (s)
∞	Surrounding/ambient

Subscripts

corr	Correction
drop	Drop
g	Gas
KY	Kurabayashi–Yang
l	Liquid
Leid	Leidenfrost
max	Maximum
o	Origin
s	Solid; surface, spreading
w	Wall

1 Introduction

The interaction of droplets with a heated solid surface in the form of the impingement of the liquid droplets

Published online: 24 April 2017

onto superheated solid surfaces have been used for many engineering applications such as in, nuclear reactor cooling, metal quenching, refrigeration cycle, electronics, and flash evaporation system. Numerous researches concerning the droplet dynamics have been carried out so far [1–6], but the observed phenomena are still unclear.

The interaction between the fluid and surface is determined by the Young–Dupree classical equation, $\boldsymbol{\sigma_{sg} = \sigma_{sl} + \sigma_{lg} cos\theta}$. Here θ is the contact angle, which is used to determine the wettability of fluid on a surface, σ is surface tension and the subscripts of *sg*, *sl*, and *lg* denote to solid–gas, solid–liquid, and liquid gas respectively. This means, the dynamics of a droplet on a heated surface depend not only on the fluid's physical property, but also on the condition of the heated solid surface and the interaction between the fluid and the surface.

In general, the term of "wettability" is defined as the interaction between the fluid and the solid surface. If the interaction is weak, the fluid will create multiple droplets on the surface and will only wet part of the surface [4]. Wettability can be categorized according to the contact angle between the fluid and the solid surface [7]. In the case of the contact angle near to zero, it is defined as perfect wetting, and for near or equal 180° from the horizontal plane, is defined as non-wetting. With water as the fluid, the term "super-hydrophilic" is used for "perfect-wetting" and "super-hydrophobic" used for "non-wetting".

The other factor that influences the dynamic of droplet during impact onto a solid surface is the Weber number (We). This number is defined as the ratio of the inertia energy to the surface tension energy. Bernardin et al. [8] categorized the Weber number into three regions (a) low We, which We < 30, (b) medium We, which 30 < We < 80, and (c) high We, which We > 80.

Concerning the impingement of a droplet onto hot surface, Bai and Gosman [9] identified the impingement regimes for a single droplet, namely, stick, rebound, spread, splash, boiling induced breakup, breakup, and rebound with breakup. During the quenching process of the metal production, the water is sprayed to the hot metal surface under low velocity, when the Weber number is near to the medium Weber number region. In this the medium We, all the regimes mentioned previously could occur for the droplet, except splashing. In some cases, due to the velocity of the impacted droplet and/or its size, the We is not high enough, but still has the effect on the cooling process. For a droplet impinging a hot surface in dry-wall regime, the Weber number equal to 30 is the criteria of rebound to rebound with breakup, and We equal to 80 is the criteria of rebound with breakup to splashing. Therefore the medium Weber number range becomes interesting to observe for the droplet impinged in wet and dry wall regime.

In the case of low We, Deendarlianto et al. [10] conducted an experimental study to observe the effect of wettability on the droplet spreading behavior during droplet impingement on the hot solid surface. The parameters of We were 5.17, 5.67, and 6.72, and the working fluid was the water. Three kinds of stainless steel surfaces, which were treated with TiO_2 and UV irradiation, were used to explain the effect of wettability. They concluded that for low Weber number, the higher the static contact angle, the lower the wetting limit temperature. The ultraviolet irradiated surface with TiO_2 did not change qualitative behavior of the evolution of spreading diameter during the droplet evaporation on a hot solid surface.

Ito et al. [11] reported the analytical and experimental behavior of the droplet when impinged onto hot surface with the temperature greater than 500 K with a Weber number range from 10 to 120. From the analytical view point, they considered that within medium We, there was no disintegration of the droplet, and the droplet remains nearly spherical after the first collision. Moreover, a good visualization of droplet evaporation was presented by The Chandra and Avedisian [3]. They used drop of n-heptane impacted onto polished stainless steel at 24–240 °C [3]. With a Weber number equal of 43, it is concluded that for temperature of hot solid surface between ambient temperature and Leidenforst temperature ($T_\infty < T_W < T_{Leid}$), the spreading ratio increases as the droplet spreads out and then decreases as the liquid begins to evaporate and/or recoil. According to their experiment, the dynamics of the droplet are strongly influenced by the solid surface temperature. Kandlikar and Steinke [12] studied the effect of the contact angle on the spreading and recoil of a droplet impinged onto hot surface. The used Weber numbers were 10, 14, 19, 29, and 58, while the surface temperatures were set from 50 to 250 °C. They proposed a correction factor to predict the droplet spreading, whereas the contact angle was taken as a parameter. A comprehensive study of droplet impingement was carried out by Lee and Ryu [9]. In their report the mapping of droplet dynamics during impingement were presented. The droplet with high Weber number tended to splash at any surface temperature. While for low We and low surface temperature, the droplet tended to stick to the surface. For medium We and high surface temperature, the droplet tended to rebound or breakup [9].

From the above facts, it is noticed that the droplet dynamics during impacting onto the hot solid surface under medium Weber number has received little attention in the past, although it is a very significant process during the metal cooling. The aim of present experimental study is to investigate the dynamics of droplet during the impact with a hot solid surface under medium Weber number. The effects of surface wettability and temperature on the droplet

spreading are presented in this present work as the main parameters.

2 Experimental apparatus and procedure

Figure 1 shows a schematic diagram of the experimental apparatus used in the present study. The heater (7), as a heat source, is attached at the bottom of the heat transfer block and insulated to avoid the heat loss. A thermostat was used to maintain the surface temperature. The temperature sensors used in the experiment are K-type thermocouples which have an uncertainty of 0.75%. In the present experiment, the variations of Weber number were obtained by the change of the drop height. The droplet diameter was 2.4 mm and the droplet was dropped from the height of 76, 84, and 92 mm, which correspond to a Weber number of 52.1, 57.6, and 63.1 respectively.

Three kinds of solid materials of heat transfer block were used: normal stainless steel (NSS), stainless steel with TiO_2 coating (UVN), and stainless steel with TiO_2 coating and radiated by ultraviolet ray (UVW). The purpose of the surface treatment of using TiO_2 coating and combined with ultra violet radiation, is to obtain the different wettability of materials. The solid surface was a cylinder with 30 mm diameter, and drilled with 3 holes at the side, where the thermocouples were placed. The distances of the holes from the surface were 5, 10, and 15 mm. The surface temperatures were varied from 60 up to 200 °C. Before the experiment, the static contact angle of droplet on each material was measured.

In each experimental run, the droplet behavior during impact onto the hot solid surface was recorded by two high speed video cameras with 1000 frame per second. The cameras have a shutter speed of 1/10,000 s, and the resolution of the video was 496 × 332 pixels. The side view of droplet was taken by first camera, which zero angle to the surface. The second video data was taken at 30° angle from the horizontal. The droplet dynamics can be observed with a 30° angle of recording camera. Meanwhile with the zero angle camera the spreading or bouncing and other visual behavior can be observed. An image processing technique was developed to analyze the video image. The analysis was carried out on the sequential images with 0° angle camera position by converting the images to binary images and measuring the droplet spreading diameter. The

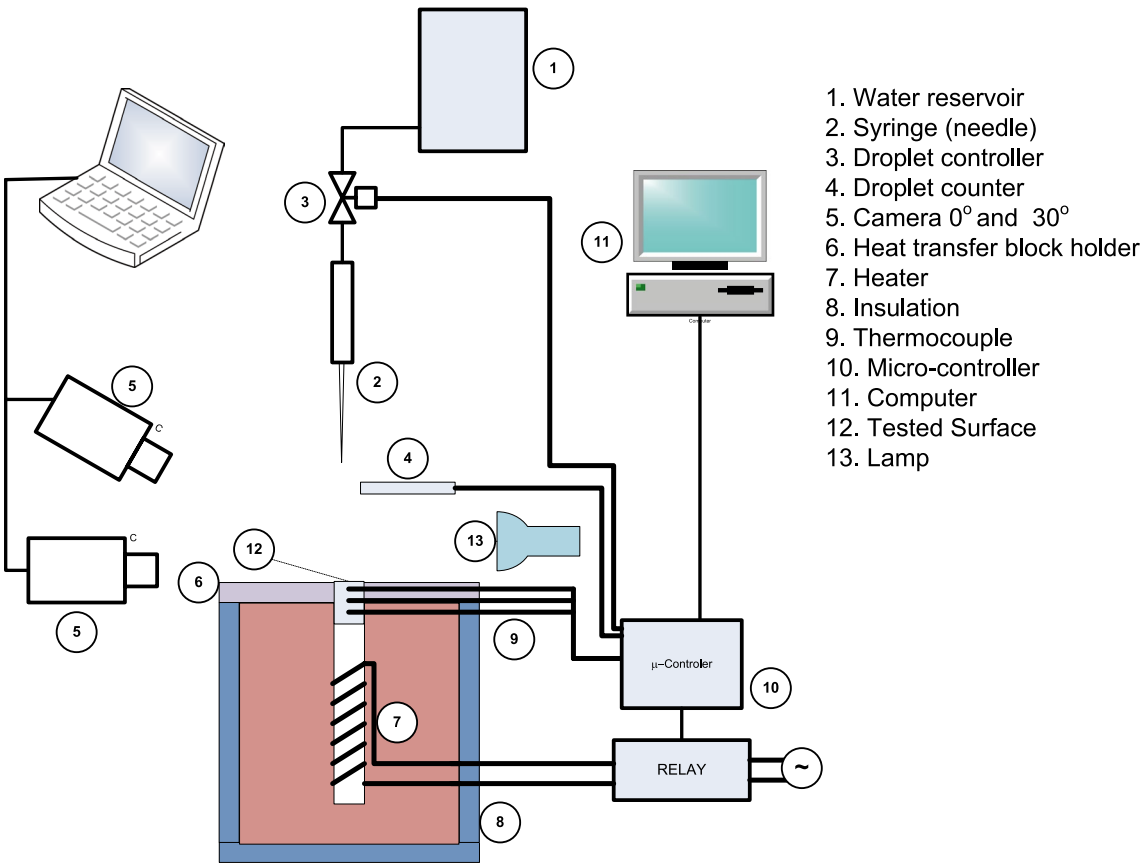

Fig. 1 Schematic diagram of experimental apparatus

image processing technique used in the present study is almost the same with that of Mitrakusuma et al. [13].

The uncertainty of the result is caused by the uncertainties of measurements or processing data. The sensitivity of sensors as mentioned are 0.75%. The data logger used to measure the temperature is a Mini Logger GL820-UM851, and has an uncertainty of 0.05% for K-type thermocouple in range −100 to 1370 °C. Other errors that should be considered is the resolution of image produced by the camera. The errors were calculated by calibrating the pixel of certain known object distance. The object with 30 mm distance has 365 pixels, then the resolution of the image is 0.082 mm/pixel. The uncertainties of Weber numbers is calculated based on the equation proposed by Taylor [14]:

For the $q = f(x_1 x_2, \ldots, x_n)$ then the uncertainty of q is:

$$\Delta q = \sqrt{\left(\frac{\partial q}{\partial x_1}\cdot \Delta x_1\right)^2 + \left(\frac{\partial q}{\partial x_2}\cdot \Delta x_2\right)^2 + \cdots + \left(\frac{\partial q}{\partial x_n}\cdot \Delta x_n\right)^2} \tag{1}$$

The definition of the Weber number is $We = \frac{\rho v^2 D}{\sigma}$, then the uncertainty of We is:

$$\Delta We = \sqrt{\left(\frac{\partial We}{\partial \rho}\cdot \Delta \rho\right)^2 + \left(\frac{\partial We}{\partial \sigma}\cdot \Delta \sigma\right)^2 + \left(\frac{\partial We}{\partial v}\cdot \Delta v\right)^2 + \left(\frac{\partial We}{\partial D}\cdot \Delta D\right)^2} \tag{2}$$

The density and surface tension are assumed constant, thus the $\Delta\rho$ and $\Delta\sigma$ are equal to zero. The previous equation can be written as:

$$\Delta We = \sqrt{\left(\frac{\partial We}{\partial v}\cdot \Delta v\right)^2 + \left(\frac{\partial We}{\partial D}\cdot \Delta D\right)^2} \tag{3}$$

Then we have:

$$\Delta We = \frac{\rho}{\sigma}\sqrt{(2\cdot v\cdot D\cdot \Delta v)^2 + \left(v^2\cdot \Delta D\right)^2} \tag{4}$$

The Δv and ΔD are the uncertainty for velocity and droplet diameter respectively. With the knowing parameters, then uncertainty of We can be calculated and tabulated as shown at Table 1.

3 Result and discussion

This work is concerned mainly with the effect of surface temperature and the wettability, which is represented by the static contact angle of fluid on the surface, on the droplet dynamics during the impacting onto a hot solid surface. The static contact angles of the tested solid surfaces were measured at ambient temperature, and the results are shown in Fig. 2. The UVW surface is near to the hydrophilic state, shown by the static contact angle which is near to zero. Meanwhile, the largest static contact angle is presented by the NSS, which is about 85.7°.

When the droplet impacts onto the hot surfaces, the shape of droplet is changed. The spreading of droplet on the solid surface becomes larger due the static contact angle. Figure 3 shows the droplet dynamics during impact onto the hot solid surfaces with temperature of 60 °C. Here We is equal to 52.1. There are two kinds of images, first

Table 1 The uncertainty of We

The height of syringe from surface, h (m)	Δh (m)	Droplet diameter, D (m)	ΔD (m)	Droplet velocity, V (m/s)	ΔV (m/s)	We	ΔWe
0.078	0.001	0.0025	0.000082	1.2368	0.0043	53.1	1.8
0.084	0.001	0.0025	0.000082	1.2835	0.0042	57.6	1.9
0.092	0.001	0.0025	0.000082	1.3432	0.0040	63.1	2.1

Then Weber number can be written as 52.1 + 1.8, 57.6 + 1.9, and 63.1 + 2.1

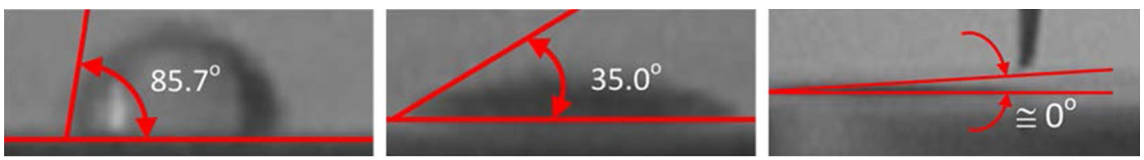

Fig. 2 Static contact angle of surfaces, **a** NSS = 85.7°, **b** UVN = 35.0°, **c** UVW ≈ 0°

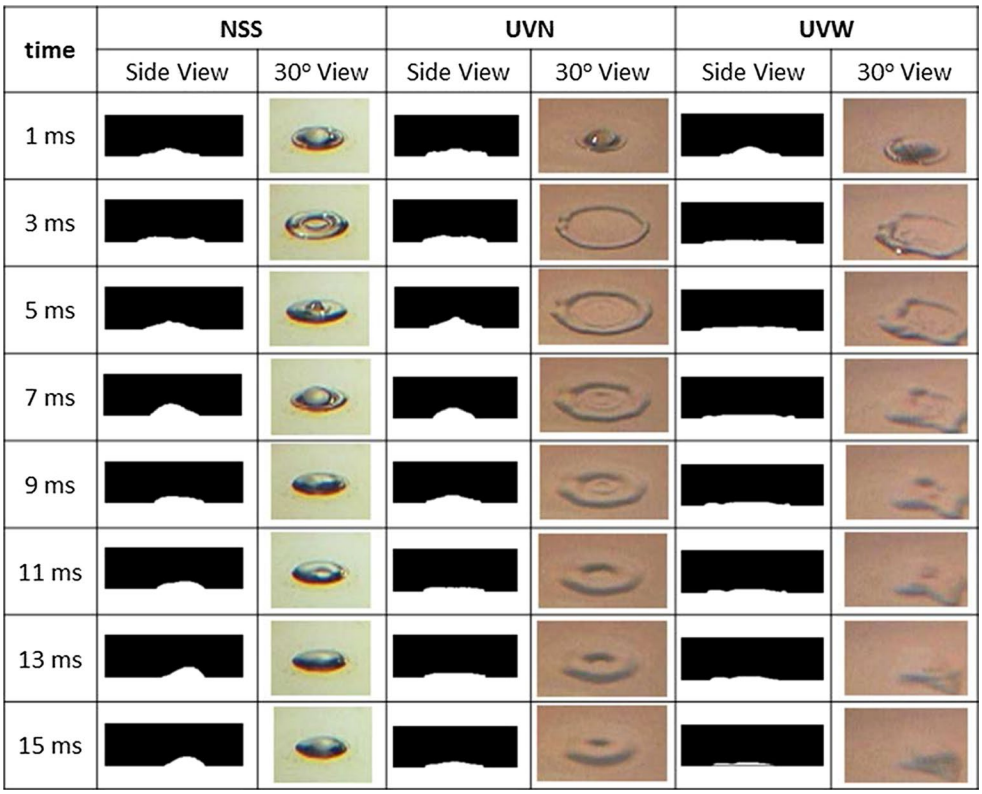

Fig. 3 Interfacial behavior at first 15 ms of the droplet after the impact onto *solid surfaces* (surface temperature was 60 °C and We = 52.1)

are the processed images from the side view, and second, on the right side, are the images taken by camera with view angle of 30° from the horizontal. After the droplet impact, the droplet experiences a change in the direction of momentum from the vertical to the radial direction. The momentum in the radial direction becomes larger. The droplet could be sticking, spreading radially, bouncing, or splashing. Other factors which influence the spreading or splashing of droplet during the impact is the wettability of liquid to surface, which is represented by contact angle as indicated by Deendarlianto et al. [10].

Still concerning Fig. 3, for NSS, the shape of the droplet at the left and right side are different. It can be seen that the droplet moves to right and left. On the first millisecond of drop, the shape of droplet seems symmetrical, but at 7 ms after the impact, the droplet tends to move to the left. On the other hand, at 13 ms, the droplet tends to move to right. This movement is repeated and become stable, due to the inhomogeneous or imbalance of force/energy inside the droplet. The forces can be from the pressure differential between inside and outside the droplet and/or momentum. This movement is clearly seen on NSS, but not at UVN or UVW.

The droplet movement did not occurr when the surface temperature is raised as shown in Fig. 4, which are 80, 100 and 120 °C. Observation of the figure indicates that the movement of droplet disappears either for NSS, UVN and UVW. Here, the wave of water droplet travels from the center to the outside, and vice versa. This periodical movement occurred for the several times after the impact, and then become stable. Under this condition, the droplet evaporation occurs only at the surface of the droplet, no bubble is detected. Next, it is noticed that at Figs. 3 and 4, no secondary droplet is produced. For the surface of NSS, at the surface temperature of 120 °C, the radial or circular ridges are formed at 3 ms after the impact. It is caused by the temperature gradient within liquid which create the surface tension gradient as reported by Chandra and Avedisian [3]. The ridges were not observed at UVN and UVW. When the surface temperature are higher than 120 °C, the droplet movement occurred again. Here, the temperature is higher than the critical heat flux (CHF) temperature, as can be seen at Figs. 5 and 6.

Figures 5 and 6 present the boiling history of the droplet under the same Weber number of 52.1. Focusing on the images at Figs. 5 and 6, whereas the surface temperatures are more than 140 °C, the droplet at certain time become unstable. This is due to the boiling process inside, especially at the bottom of the droplet contacted on surface. At Fig. 5a–c, after the droplet impacted to the hot solid surface, the secondary droplet is formed and dispersed to surrounding of the droplet (cf. at t = 118 ms of NSS, t = 104 ms of UVN, and t = 27 ms of UVW). During this condition, the bubbles which are formed at the bottom, are

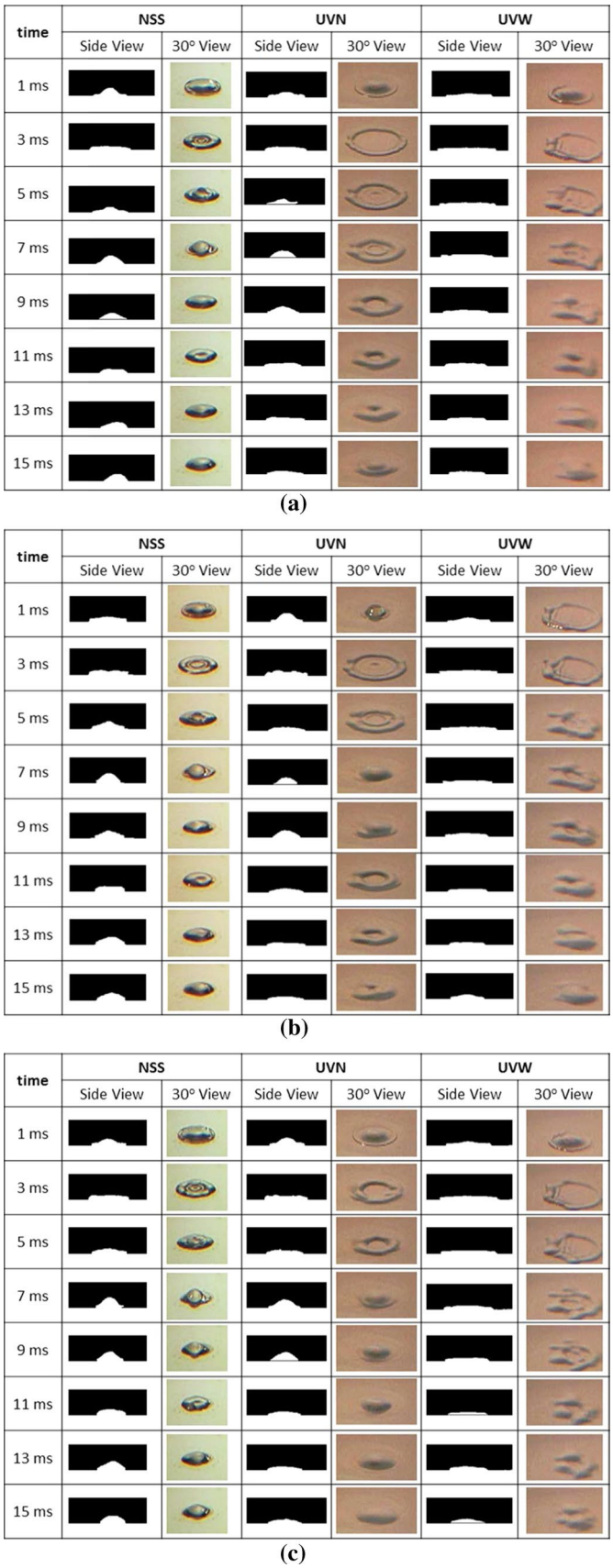

Fig. 4 Interfacial behavior at first 15 ms of the droplet after the impact onto *solid surfaces* (surface temperature were 80, 100, and 120 °C and We = 52.1). **a** Surface temperature = 80 °C. **b** Surface temperature = 100 °C. **c** Surface temperature = 120 °C

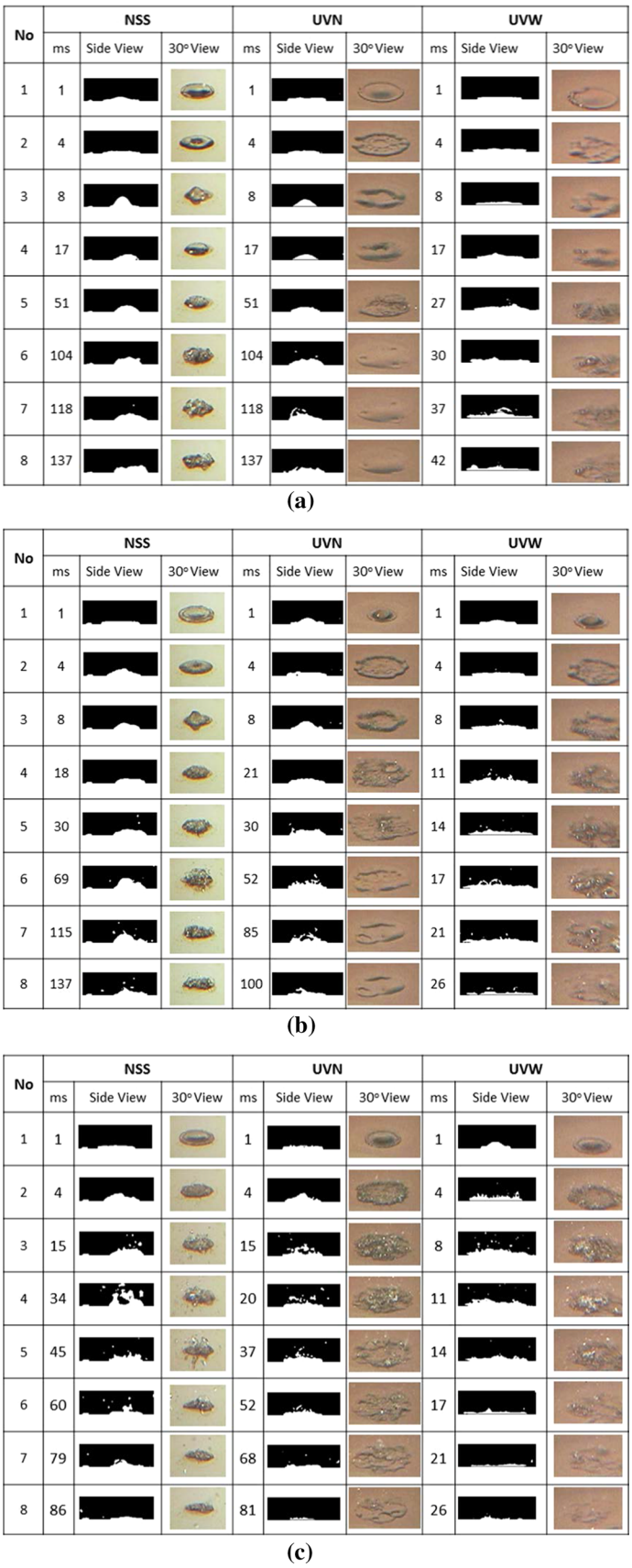

No	NSS			UVN			UVW		
	ms	Side View	30° View	ms	Side View	30° View	ms	Side View	30° View
1	1			1			1		
2	4			4			4		
3	8			8			8		
4	17			17			17		
5	51			51			27		
6	104			104			30		
7	118			118			37		
8	137			137			42		

(a)

No	NSS			UVN			UVW		
	ms	Side View	30° View	ms	Side View	30° View	ms	Side View	30° View
1	1			1			1		
2	4			4			4		
3	8			8			8		
4	18			21			11		
5	30			30			14		
6	69			52			17		
7	115			85			21		
8	137			100			26		

(b)

No	NSS			UVN			UVW		
	ms	Side View	30° View	ms	Side View	30° View	ms	Side View	30° View
1	1			1			1		
2	4			4			4		
3	15			15			8		
4	34			20			11		
5	45			37			14		
6	60			52			17		
7	79			68			21		
8	86			81			26		

(c)

Fig. 5 Interfacial behavior at first 15 ms of the droplet after the impact onto *solid surfaces* (surface temperature were 140, 160, and 180 °C and We = 52.1) **a** Surface temperature = 140 °C. **b** Surface temperature = 160 °C. **c** Surface temperature = 180 °C

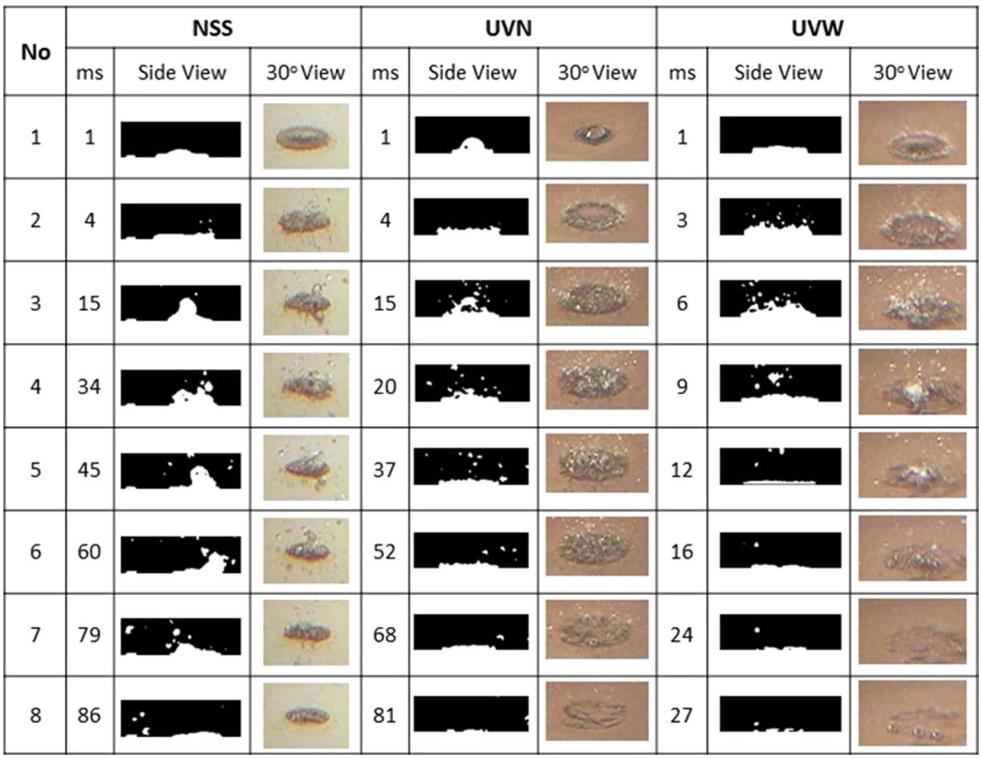

Fig. 6 Interfacial behavior at first 15 ms of the droplet after the impact onto *solid surfaces* (surface temperature was 200 °C and We = 52.1)

coalesced to each other, and fly to the upper part of droplet, and then collapsed, and produce small droplet. The obtained results are in a good agreement with Mitrakusuma et al. [15], who investigated the boiling phenomena around the onset of nucleate boiling.

Furthermore, after the droplet break-up appeared, many secondary droplets were produced and jetted from the entire area of the surface. The time when the secondary droplet, in the form of small water mist/particle, occurs is earlier for higher surface temperature. This explanation, is in a good agreement with those of McHale and Garimella [16], Collier and Thome [17], which reported that the bubble is formed when the surface temperature is higher than saturation temperature. As the surface temperature rises, the time of debris becomes earlier, e.g. at 160 °C, t = 8 ms of NSS, t = 8 ms of UVN, and t = 4 ms of UVW. Moreover, the effect of surface wettability are not significantly seen for a higher surface temperature, cf. at 200 °C, as can be seen clearly at Fig. 6.

Figure 7 shows the effect of the Weber number on the spreading and the shape of the droplet on the NSS surface at 200 °C. In the figures, only the main part of droplet is shown for the side view. All the droplets for all the tested surfaces begin to boil at 1 ms after the impact, and then the secondary droplet appears, which mean the droplets were broken up. Next, the secondary droplets splash around the droplet. As the time goes by, the decrease of droplet volume can be seen clearly as shown by the droplet diameter.

For the higher We, the wetting diameters and the evaporation rate are higher than that of the lower We. It is possible due to the larger contact area as shown in Fig. 7. At a higher We, when the droplet impacts to the hot solid surface, the droplet spreading diameter is larger than that of the lower We. As an illustration, with the We = 52.1, the diameter of droplet at 5 ms is 5.84 mm, and at 20 ms is 5.52 mm. The average diameter reducing rates of droplet for this period is 0.027 mm/ms. Meanwhile, the average diameter reducing rates from 5 to 20 ms, are 0.125 mm/ms for We = 63.1 and 0.050 mm/ms for We = 57.6. This can be concluded that the higher We, the higher diameter reducing rate, the faster the evaporation rate.

The history of droplet spread for the first ten milliseconds after impact is shown in Fig. 8. The figure shows that the droplet spreading diameter increases with the increase of We, especially for NSS. The maximum droplet spreading diameter is 10 mm for We = 63.1, 8.5 mm for We = 57.6 and 6.8 mm for We = 52.1, as shown at Fig. 8a. Meanwhile for UVN, the effect of We on the droplet spread is not significant, as shown at Fig. 8b. Figure 8b the data from Deendarlianto et al. [10] at the low Weber number of 5.1. Observation of the figure indicates that at a higher We, the droplet tends to oscillate, meanwhile it does not exist at lower We. This figure proves that the inertia force, represented by We, plays an important role during the droplet impact on the hot solid surface. On the other hand the effect

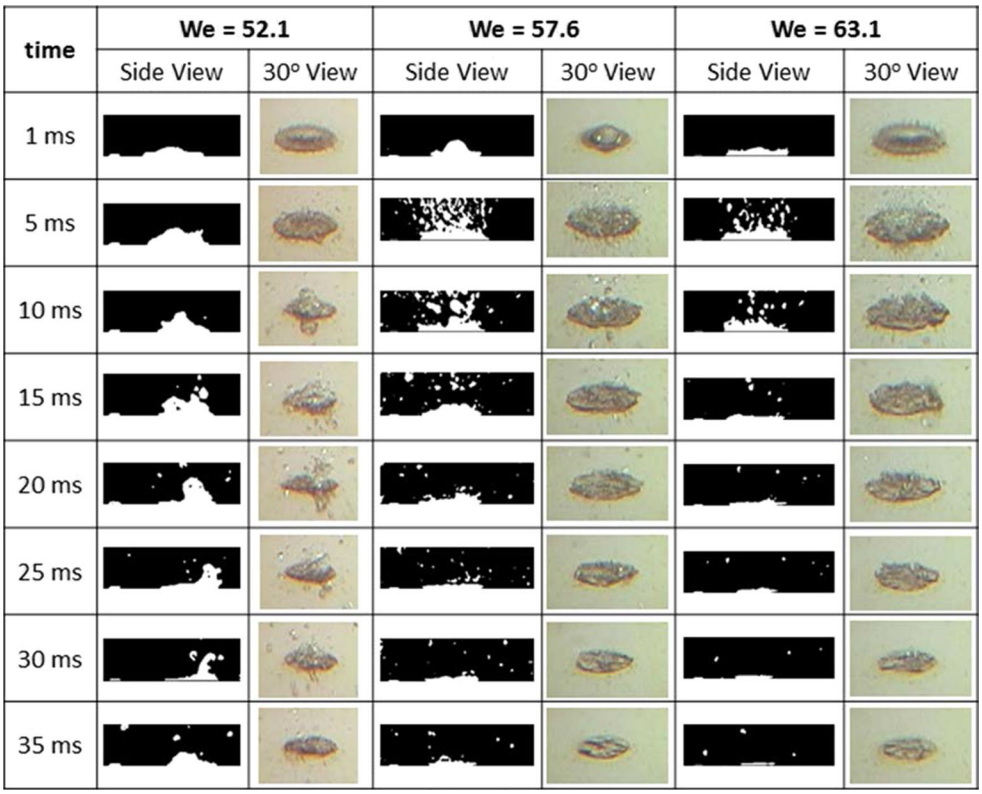

Fig. 7 The behavior of *droplet* after the impact onto *solid surfaces* (Weber number 52.1, 57.6, and 63.1 and surface temperature 200 °C)

of the surface temperature is also insignificant. According to Lee and Ryu [9], for the low Weber number (<5), it has low impact energy, and the droplet tends to stick to the surface. The oscillation of droplet has been studied by Manglik et al. [18]. The basic equation proposed by Manglik was a second order differential equation, which had the general solution of:

$$y(t) = e^{-(\alpha t/2)}\left[A\ cos(\gamma t) + B\ sin(\gamma t)\right] \tag{5}$$

where y(t) is the spreading of droplet, $\alpha = (c/m)$ is viscous damping factor, c is damping coefficient, m is droplet mass, $\gamma = \sqrt{\omega^2 - (\alpha/2)^2}$, ω is the frequency, $A = y(0)$ is the initial displacement, and $B = \frac{1}{\gamma}\left\{\dot{y}(0) + \frac{\alpha}{2}y(0)\right\}$ [18]. The solutions proposed, did not included the effect of solid surface temperature. Further investigation of the oscillation of the droplet and the effect of surface temperature on droplet dynamics should be carried out.

By comparing Fig. 8a, c, it can be seen that the oscillation disappears at low static contact angle. After the impact, it is observed that it behavior is similar, but for higher temperatures, the droplet begins to boil and evaporate. This can be seen by the irregular droplet shape and the droplet spreading diameter. Therefore, it is concluded that the surface temperature has a minor effect on the droplet spread diameter during the droplet impacted to hot solid surfaces if the static contact angle is low. For UVW the droplet spread diameter is almost the same as that of the other tested We. The obtained phenomena appeared also for very low Weber number, as reported by Deendarlianto et al. [10]. This means that the droplet spread diameter is more influenced by wettability than We for the solid surface near the super-hydrophilic condition. On the other hand, for the surface with low wettability, the We has a strong influence on the droplet spread.

The maximum droplet spread (D_{max}) is shown in Fig. 9, and the remarks can be given as follow. For We = 52.1, all the tested surfaces show a constant maximum droplet-spreading diameter, even if the surface temperature is changed. The D_{max} of UVW reaches the highest value compared to that of NSS and UVN. At the highest Weber number (We = 63.1), the maximum droplet spread is almost the same for all the tested surfaces. Thus, it can be concluded that for high We, the surface treatment has no significant effect on D_{max}.

The spreading diameter is marked by the spreading ratio (β), and is defined as:

$$\beta = \frac{D}{D_o} \tag{6}$$

Here D is the droplet spreading, and D_o is the initial diameter of droplet before impacted to the solid surface. The maximum spreading ratio can be obtained at the maximum droplet spreading diameter, and expressed as:

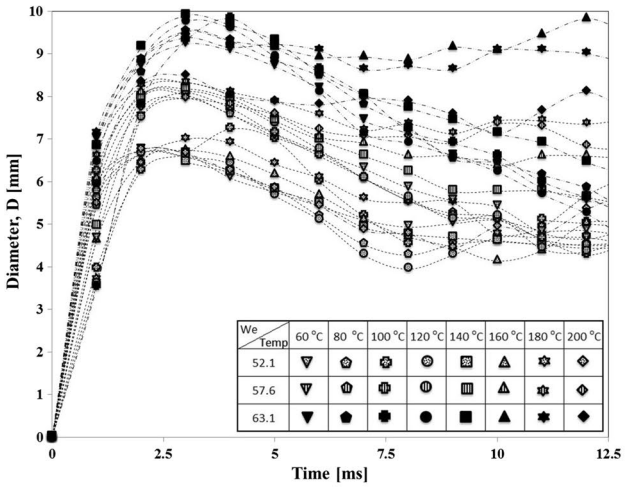

(a)

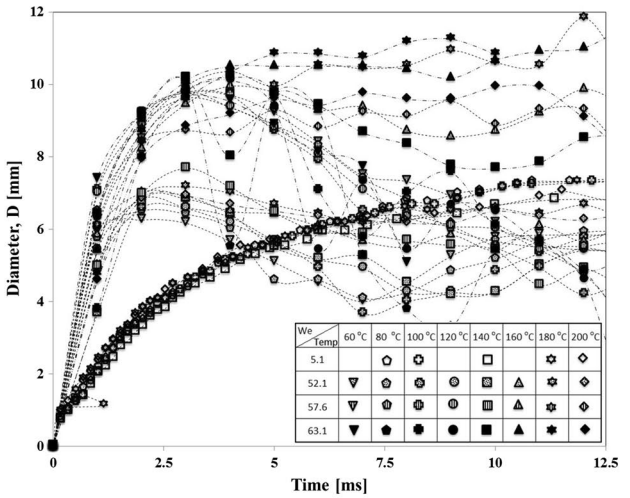

(b)

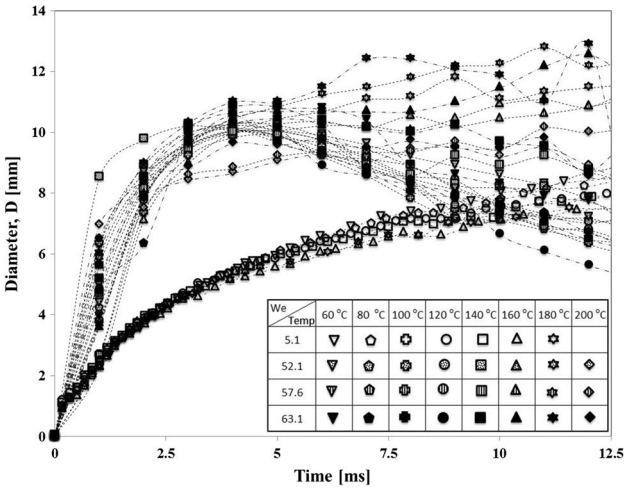

(c)

Fig. 8 *Droplet* spreading at first 12.5 ms, for NSS, UVN, and UVW, were compared to lower Weber number (We = 5.1, data taken from Deendarlianto [10]). **a** NSS. **b** UVN. **c** UVW

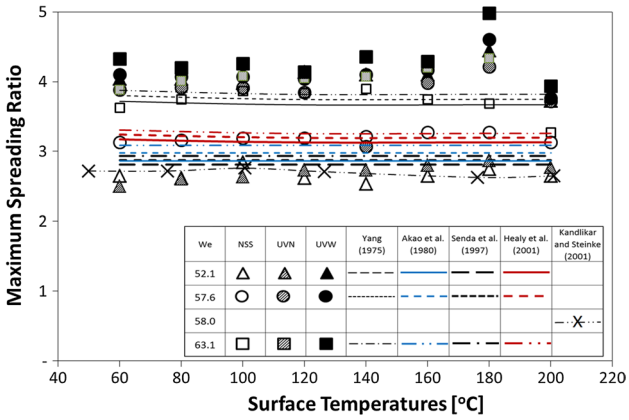

Fig. 9 Maximum spreading ratio of droplet on different We number

$$\beta_{max} = \frac{D_{max}}{D_o} \tag{7}$$

Several equations were proposed to predict the maximum spreading diameter of a droplet impingement onto a hot solid surface, as summarized in Table 2. The available empirical correlations contain the Weber number, fluid viscosity, fluid contact angle, and Reynolds number as the parameters. The comparison of the available correlations with the present experimental data is presented in Fig. 9. It can be seen that for NSS, the β_{max} obtained from the present experimental study has a good agreement with available correlations and the data from Kandlikar and Steinke [12]. Meanwhile, for UVN and UVW the available correlations over predicts the experimental results. This is possibly due to the static contact angle playing an important role while it is generally not considered in the available correlations. Although Healy et al. correlation [22] includes the static contact angle in their experimental correlation, the correlation under predicts the experimental data. It is possible due to their correlation base only under the contact angle of 45° and 70°. Therefore, further systematic experimental studies are needed to study the effect of static contact angle in order to develop the understanding on their influence on the boiling phenomena.

Figure 10 shows the evaporating time of single droplet impacting onto hot solid surface. In the figure, the right side is an enlargement of the graph for certain points where the evaporating time is very small. The evaporating time is defined as the time of the droplet still exists on the solid surface during the evaporation. When a droplet is observed to bounce or detach from surface, caused by the thin film of vapor produced during evaporation at the bottom of the droplet, the temperature at this condition is called wetting limit temperature [23]. From the experiment, it is observed that the wetting limit temperature is around 200 °C.

Table 2 Different proposed empirical correlation to predict the maximum spreading ratio

No.	Correlation	Researcher
1	$\frac{We}{2} = \frac{3}{2}\beta_{max}^2\left[1 + \frac{3We}{Re}\left(\beta_{max}^2 \ln(\beta_{max} - \frac{\beta_{max}^2 - 1}{2})\right)\left(\frac{\mu_{drop}}{\mu_{wall}}\right)^{0.14}\right] - 6$ (8)	Yang [19]
2	$\beta_{max} = 1,0 + 0.463We^{0.345}$ (9)	Senda et al. [20]
3	$\beta_{max} = 0.613We^{0.39}$ (10)	Akao et al. [21]
4	$\beta_{max,corr} = \beta_{max,KY}\left(\frac{45}{\theta}\right)^{0.241}$ (11)	Healy et al. [22]

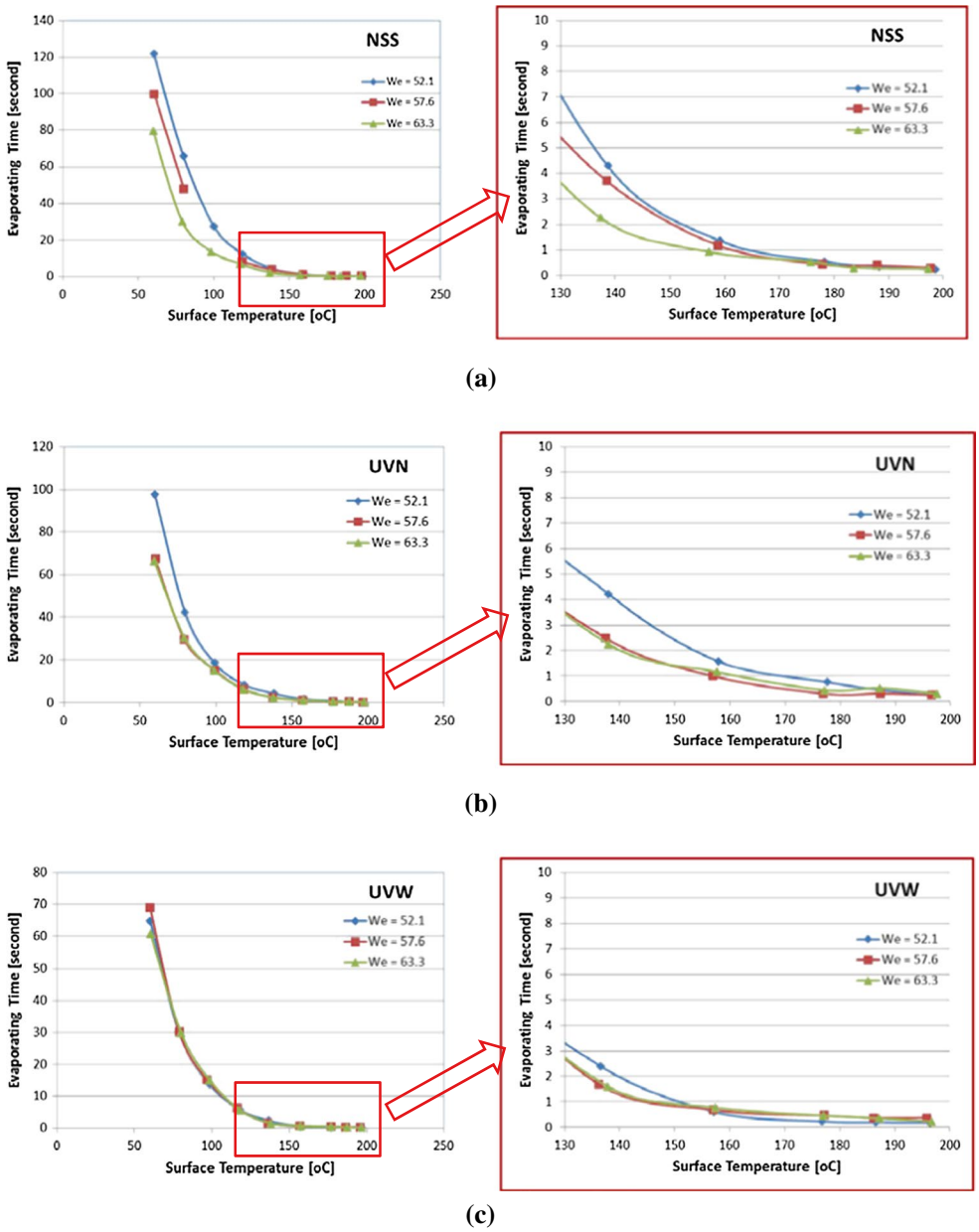

Fig. 10 Evaporating time

From Fig. 10, it can be seen that for the temperature below 120 °C, evaporating time decreases immediately but for the temperature higher than 120 °C the evaporating time decreases slowly. The effect of We on the evaporation time of NSS is significant, whereas the evaporation time decrease as the We increases. At the surface temperature of 120 °C for NSS (We = 52.1; 57.6; and 63.3), the evaporating times are 4.3, 3.7, and 2.8 s respectively. Meanwhile, for UVN the evaporating times are 4.21, 2.5, 2.26 s. These data show that We number plays a significant role on evaporating time. For higher We, the droplet spread diameter is larger, thus the contact area is also higher. This result is a shorter time evaporation. On the other hand, this phenomena did not occur for UVW, as discussed previously. Therefore, the We has no significant effect on the droplet spread diameter for the super hydrophilic surfaces.

From the view point of heat transfer, if Q is the heat to evaporate a droplet, and q is the evaporation heat transfer rate, then the evaporating time can be defined as $\tau = Q/q$. Here it is assumed that the heat transfer is convection heat transfer, and it can be written as $q = h \cdot A \cdot (T_s - T_w)$. Here A is the droplet contact area to the surface, and then evaporating time can be written as:

$$\tau = \frac{4Q}{\pi\beta^2 D_o^2 h(T_s - T_w)} \tag{12}$$

The last equation shows that the evaporation time becomes shorter with the increase of β, and that is the reason why UVW has the shortest evaporation time.

4 Concluding remark

The experimental study on the dynamic of a droplet impacting onto hot solid surfaces under medium Weber number was carried out. The calculation of the surface wettability was obtained by the coating of the stainless steel with TiO_2 and ultraviolet irradiation. The surface temperature was varied from 60 to 200 °C. Their effects on the droplet spreading were studied, and the results are summarized as follows:

1. The wettability has a significant effect on the droplet spreading. The higher the wettability, the larger the droplet spreading during the droplet impacting onto hot solid surface.
2. The effect of We is also significant on the droplet spreading ratio for NSS and UVN. The larger the Weber number, the higher the droplet spreading ratio. For the UVW, the effect of We is insignificant on the droplet spreading.
3. For the medium Weber numbers, the surface temperature has a significant role on the evaporation time. The higher the surface temperature, the shorter the evaporating time.
4. The available experimental correlation could not correlate the experimental data as the effect of the surface wettability under medium Weber number was not considered. This means that further experimental works are needed to clarify the effect of surface wettability in some more detail, especially the effect of contact angle on the spreading diameter.

Acknowledgements This research is partly supported by National Competitive Research Program Grant of Directorate of Higher Education, Ministry of Research, Technology and Higher Educations Republic of Indonesia.

References

1. Grissom WM, Wierum FA (1981) Liquid spray cooling of a heated surface. Int J Heat Mass Transf 24:261–271. doi:10.1016/0017-9310(81)90034-X
2. Bechtel SE, Bogy DB, Talke FE (1981) Impact of a liquid drop against a flat surface. IBM J Res Dev 25:963–971
3. Chandra S, Avedisian CTT (1991) On the collision of a droplet with a solid surface. Proc R Soc A Math Phys Eng Sci 432:13–41. doi:10.1098/rspa.1991.0002
4. Bernardin JDID, Mudawar I, Walsh CB et al (1997) Contact angle temperature dependence for water droplets on practical aluminum surfaces. Int J Heat Mass Transf 40:1017–1033. doi:10.1016/0017-9310(96)00184-6
5. Deendarlianto, Takata Y, Hidaka S, Kohno M (2008) The effect of contact angle on evaporation of water droplet on a heated solid surface. In: Fifth international conference on transport phenomena in multiphase systems. Bialystok, Poland, pp 59–64
6. Eggers J, Fontelos MA, Josserand C, Zaleski S (2010) Drop dynamics after impact on a solid wall: theory and simulations. Phys Fluids 22:1–14. doi:10.1063/1.3432498
7. Coursey JS (2007) Enhancement of spray cooling heat transfer using extended surfaces and nanofluids. University of Maryland
8. Bernardin JD, Stebbins CJ, Mudawar I (1997) Mapping of impact and heat transfer regimes of water drops impinging on a polished surface. Int J Heat Mass Transf 40:247–267. doi:10.1016/0017-9310(96)00119-6
9. Lee SY, Ryu SU (2006) Recent progress of spray-wall interaction research. J Mech Sci Technol 20:1101–1117. doi:10.1007/BF02916010
10. Deendarlianto Takata Y, Hidaka S et al (2014) Effect of static contact angle on the droplet dynamics during the evaporation of a water droplet on the hot walls. Int J Heat Mass Transf 71:691–705. doi:10.1016/j.ijheatmasstransfer.2013.12.066
11. Ito T, Takata Y, Mousa MMM (1992) Studies on the water cooling hot surfaces (analysis of spray cooling in the region associated with film boiling). Jpn Soc Mech Eng 35:589–598
12. Kandlikar SG, Steinke ME (2001) Contact angles of droplet during spread and recoil after impinging on a heated surface. Trans IChemE 79:491–498
13. Mitrakusuma WH, Deendarlianto Kamal S et al (2015) Determining contact angle and spreading velocity of a droplet impacted hot solid surface. Appl Mech Mater 771:183–186. doi:10.4028/www.scientific.net/AMM.771.183

14. Taylor JR (1997) An introduction to error analysis, the study of uncertainties in physical measurement, 2nd edn. University Science Books, Sausalito
15. Mitrakusuma WH, Deendarlianto Kamal S et al (2016) Experimental investigation on the phenomena around the onset nucleate boiling during the impacting of a droplet on the hot surface. AIP Conf Proc 50002:50002–1–50002–8. doi:10.1063/1.4949305
16. McHale JP, Garimella SV (2010) Bubble nucleation characteristics in pool boiling of a wetting liquid on smooth and rough surfaces. Int J Multiph Flow 36:249–260. doi:10.1016/j.ijmultiphaseflow.2009.12.004
17. Collier JG, Thome JR (1994) Convective boiling and condensation, 3rd edn. Clarendon Press, Oxford
18. Manglik RM, Jog MA, Gande SK, Ravi V (2013) Damped harmonic system modeling of post-impact drop-spread dynamics on a hydrophobic surface. Phys Fluids. doi:10.1063/1.4819243
19. Yang WJ (1975) Theory on vaporization and combustion of liquid drops of pure substances and binary mixtures on heated surfaces. Technical report 535, Institute of Space and Aeronautical Science, University of Tokyo
20. Senda J, Kanda T, Ai-roub M, Farrell PV (1997) Modeling spray impingement considering fuel film formation on the wall. SAE Trans J Eng 106:37–51. doi:10.4271/970047
21. Akao F, Araki K, Mori S, Moriyama A (1980) Deformation behaviors of a liquid droplet impinging onto hot metal surface. Trans Iron Steel Inst Jpn 20:737–743
22. Healy WM, Hartley JG, Abdel-Khalik SI (2001) Surface wetting effects on the spreading of liquid droplets impacting a solid surface at low Weber numbers. Int J Heat Mass Transf 44:235–240. doi:10.1016/S0017-9310(00)00097-1
23. Hidaka S, Yamashita A, Takata Y (2006) Effect of contact angle on wetting limit temperature. Heat Transf Res 35:513–526. doi:10.1002/htj.20128